

# Fatty Acid Ratios as Parameters to Discriminate Between Normal and Tumoral Cells and Compare Drug Treatments in Cancer Cells

Antonella Rosa,\* Mariella Nieddu, Federica Pollastro, and Cristina Piras

The fatty acid (FA) composition of cell membranes represents a metabolic biomarker. However, the FA profile reproducibility in cell cultures remains a significant challenge. In this study, cell FA ratios are validated as metabolic markers alternative to cell FA. To this goal, cell samples belonging to cancer HeLa cells and normal 3T3 fibroblasts, from various experimental sets, are analyzed by a high-performance liquid chromatography system coupled with a photodiode array detector and evaporative light scattering detector (HPLC-DAD/ELSD), and the ratios among the main FA are calculated. Principal component analysis (PCA) separately performed on FA and FA ratio data indicates similar clustering of cell samples concerning the cell type. Moreover, similar scores values  $t[1]$  and  $t[2]$  and graphical distances are calculated in the PCA plots separately performed on FA and FA ratios measured in cancer HeLa cells subjected to various antitumoral compounds. Last, PCA applied to selected FA ratios measured in various cell lines, obtained in similar experimental conditions, allows to discriminate between normal and tumoral cells. The results substantiate FA ratios as a cell-specific fingerprint, characterized by reproducibility across intra-laboratory conditions, useful for cell characterization, discrimination between normal and tumoral cells, and the comparison of different drug treatments.

**Practical Applications:** The reproducibility of the fatty acid (FA) profile in cell cultures remains a significant challenge. Results obtained from this study improve knowledge about the role of the FA ratio profile as a cell-specific fingerprint characterized by reproducibility across intra-laboratory conditions. The characterization of the specific FA ratio profile of a cell culture, under standardized experimental conditions, can facilitate the comparative evaluation of cell data sets for nutritional, metabolic, and pharmacological studies, overcoming differences in cell culture conditions and FA extraction/analytical procedures.

## 1. Introduction

Lipids have structural, energy, signalling, and immunoregulatory functions, playing different important roles at cellular, tissue, and organismal level.<sup>[1,2]</sup> Fatty acids (FA) are the main building blocks of numerous lipid species and contribute to metabolic homeostasis and physiological functions in normal cells.<sup>[3–7]</sup> Cell membrane FA composition is tightly regulated and can be considered a homeostatic, metabolic, and nutritional biomarker.<sup>[4,5]</sup> Therefore, alterations in tissue and cell FA composition are amply studied as biomarkers of pathological conditions.<sup>[6,8,9]</sup> In particular, the deregulation of lipid and FA metabolism is one of the most important metabolic hallmarks of cancer cells.<sup>[1,3,7–9]</sup> Cancer cells show an increased de novo FA biosynthesis and exogenous FA uptake that sustains their rapid proliferative rate and provides an essential energy source during metabolic stress conditions.<sup>[1,3,7–9]</sup> FA profile alterations in cancer tissues and/or cells have been proposed as diagnostic tools for colorectal<sup>[10]</sup> and breast<sup>[11]</sup> cancer. Higher levels of monounsaturated FA (MUFA), mainly oleic acids 18:1 *n*-9, and increased amounts of palmitic acid 16:0, as the main product of de novo lipogenesis, have been measured in cancer cells and tissues.<sup>[3,7,10,12]</sup> Targeting altered lipid metabolic pathways (such as FA biosynthesis/desaturation, phospholipids, and cholesterol metabolism) has become a

 The ORCID identification number(s) for the author(s) of this article can be found under <https://doi.org/10.1002/ejlt.202200128>

© 2023 The Authors. European Journal of Lipid Science and Technology published by Wiley-VCH GmbH. This is an open access article under the terms of the Creative Commons Attribution License, which permits use, distribution and reproduction in any medium, provided the original work is properly cited.

DOI: 10.1002/ejlt.202200128

A. Rosa, M. Nieddu, C. Piras  
Department of Biomedical Sciences  
University of Cagliari  
Cittadella Universitaria  
SS 554, Km 4.5, Monserrato, Cagliari 09042, Italy  
E-mail: anrosa@unica.it

F. Pollastro  
Department of Pharmaceutical Sciences  
University of Eastern Piedmont  
Largo Donegani 2, Novara 28100, Italy  
F. Pollastro  
PlantaChem Srls  
via Amico Canobio 4/6, Novara 28100, Italy

promising anti-cancer strategy.<sup>[8,9,13,14]</sup> Many anticancer compounds are inhibitors of fatty acid synthase (FAS), a multi-enzyme that catalyses de novo synthesis of 16:0,<sup>[3,7]</sup> and stearoyl-CoA desaturase (SCD), an enzyme that inserts a double bond in the  $\Delta^9$  position of saturated FA (SFA) to generate MUFA.<sup>[9,12]</sup>

Traditional in vitro cell culture methods using a 2D monolayer have become a standard technology in life sciences,<sup>[7,15,16]</sup> representing a defined model system for studying cell behavior in a controlled environment.<sup>[16]</sup> Cultured cells are amply used to study differences in FA metabolism between normal and cancer cells and to evaluate the effect of drugs in modulating FA profile and regulating the structure of the membrane.<sup>[2,5]</sup> The analysis of FA composition in cultured cell models requires different steps, including solvent-based extraction, saponification, derivatization of lipid components, and chromatography techniques for the identification/quantification of free FA or their derivatives.<sup>[2]</sup> Therefore, the reproducibility, reliability, and variability of the cell FA data across intra-laboratory conditions and independent laboratories remain a significant challenge that depends on multiple factors such as cell culture conditions and FA extraction/analytical procedures.<sup>[17,18]</sup> Moreover, the reliability of the cell data across independent laboratories is complicated by differences in units in which FA data are provided (as mass percentages,  $\mu\text{g}$  per plate, or  $\mu\text{g mg}^{-1}$  protein).<sup>[19]</sup> Recent studies have proposed FA ratios as a suitable way to effectively replace the original FA data set.<sup>[19]</sup> FA ratios are believed to have sub-compositional coherence because the ratio between two specific FA is a dimensionless quantity and remains the same whatever other FA are included, with or without normalization.<sup>[19]</sup> The determination of arachidonic:eicosapentaenoic acid ratio (20:4 *n*-6/20:5 *n*-3) in whole blood lipids has been proposed as a rapid and reliable method for determining *n*-3 FA status, generally considered as a biomarker for different pathologies.<sup>[20]</sup> Moreover, lower values of 20:4 *n*-6/20:5 *n*-3 and 16:0/18:1 *n*-9 ratios have been measured in cancer cell lines concerning normal counterparts.<sup>[21]</sup>

Starting from all these considerations, the main objective of this study was to explore and validate, under intra-laboratory conditions and through a biochemical and chemometric approach, the potential use of the FA ratio profile as a data set alternative to the total FA profile for cell characterization, discrimination between normal and cancer cells, and for the quantitative comparison of drug treatments in the same cancer cell line. Initially, cell samples belonging to two different cell lines (cancer HeLa cells and normal 3T3 fibroblasts), obtained from different standardized experimental sets, were characterized for their FA and FA ratio profiles. The cultured cells used in this study were chosen as amply utilized as cell models for assessing the lipid modulatory effects of natural/synthetic FA and anticancer compounds.<sup>[5,22–25]</sup> Analysis of cell FA was performed by a high-performance liquid chromatography system (HPLC) coupled with a photodiode array detector (DAD) and evaporative light scattering detector (ELSD). FA ratio profile was also measured in cancer HeLa cell samples treated with several antitumoral compounds (zerumbone, eupatilin, artemetin, and its derivatives 8-prenyl artemetin and 5-*O*-prenyl artemetin) obtained from previous experimental sets.<sup>[22–25]</sup> These natural compounds were selected based on their ability to affect lipid/FA profile in cancer cells, maybe acting as inhibitors of FAS and SCD enzymes.<sup>[22–25]</sup> Principal com-

ponent analysis (PCA), a statistical procedure amply used to summarize and compare the total FA profile of oils,<sup>[26]</sup> marine organisms,<sup>[19]</sup> and cell lines/tissues,<sup>[27]</sup> was comparatively applied to cell FA and FA ratio data to validate the role of FA ratios as useful reproducible metabolic parameters for cell characterization/discrimination, and the comparison of different drug treatments, alternative to total FA profile. Last, a small set of selected FA ratios was calculated for other cell lines, previously cultured/analyzed in our laboratories under similar experimental conditions, and compared by PCA in the perspective to assess their role in discriminating between cancer and normal cells.

## 2. Experimental Section

### 2.1. Chemicals and Reagents

Standards of fatty acids (FA) were obtained from Sigma–Aldrich (Milan, Italy). Cell culture materials were purchased from Invitrogen (Milan, Italy). All the chemicals used in this study were of analytical grade. According to the literature, zerumbone was isolated from the essential oil of shampoo ginger<sup>[22]</sup> and eupatilin from the Swiss chemotype of *Artemisia umbelliformis* Lam.<sup>[23]</sup> Artemetin was purified from the aerial part of *Artemisia absinthium*<sup>[24]</sup> and their derivatives (5-*O*-prenyl and 8-prenyl artemetin) were synthesized as previously reported.<sup>[25]</sup>

### 2.2. Cell Cultures

Human adenocarcinoma HeLa cell line and mouse 3T3 fibroblasts were obtained from the American Type Culture Collection (ATCC, Rockville, MD). Cells were grown in Dulbecco's modified Eagle's medium (DMEM) with high glucose, supplemented with 2 mM L-glutamine, penicillin (100 units per mL)—streptomycin (100  $\mu\text{g mL}^{-1}$ ), and foetal calf serum (FCS) (10% v/v), at 37 °C in a 5% CO<sub>2</sub> incubator. Subcultures of HeLa and 3T3 cells were grown in T-75 culture flasks and passaged with a trypsin-EDTA solution. Normal VERO cells, cancer undifferentiated Caco-2 cells, differentiated Caco-2 cells, and B16F10 cancer cells were used for FA ratio comparison. FA data of selected cells were obtained from previous experimental sets conducted under standardized experimental conditions (Table S1, Supporting Information, and citations therein). Morphology evaluation of cancer HeLa cells and normal 3T3 fibroblasts was performed by microscopic analysis with a ZOE Fluorescent Cell Imager (Bio-Rad Laboratories, Inc., California, USA).

### 2.3. Determination of Cell Fatty Acid Profile

Cancer HeLa cells and 3T3 fibroblasts were plated in Petri dishes (at a density of 10<sup>6</sup> cells per 10 mL of complete culture medium) and cultured for 48 h. Cells were then washed with PBS to remove dead cells, scraped, and centrifuged (at 2000 rpm at 4 °C for 10 min). Cell pellets were separated from the supernatants and then used for the extraction of lipid compounds. Four experiments (indicated as Exp. A, Exp. B, Exp. C, and Exp. D) with several replicates were performed for each cell line at different times

(during 2 years) with the same experimental conditions. Cancer HeLa cells were also treated, in fresh culture medium, with several anticancer drugs in different experimental sets conducted at different times, as previously reported: zerumbone (treatment A; 10, 50, and 100  $\mu\text{M}$ ),<sup>[22]</sup> eupatilin (Treatment B; 10, 25, and 50  $\mu\text{M}$ ),<sup>[23]</sup> artemetin (Treatment C; 10, 25, and 50  $\mu\text{M}$ ),<sup>[24]</sup> and its derivatives 8-prenyl artemetin and 5-O-prenyl artemetin (Treatment D, 25  $\mu\text{M}$ ).<sup>[25]</sup> After treatments, cells were washed, scraped, and centrifuged and cell pellets were used for the extraction of lipid compounds.

#### 2.4. Extraction and Analysis of Cell Fatty Acids

Total lipids were extracted from 3T3 fibroblast and HeLa cell pellets with the chloroform/methanol/water 2:1:1 mixture as previously reported.<sup>[22]</sup> Dried chloroform fractions after cell pellet extraction, dissolved in ethanol, were subjected to mild saponification as reported.<sup>[22]</sup> Analyses of unsaturated (DAD detection, 200 nm) and saturated (ELSD detection) FA, obtained from cell lipid saponification, were carried out with a mobile phase of acetonitrile/water/acetic acid (75/25/0.12, v/v/v), at a flow rate of 2.3 mL min<sup>-1</sup>, and data were collected and analyzed using the Agilent OpenLAB Chromatography data system, as previously described.<sup>[22]</sup> Calibration curves of FA were constructed using standards and were found to be linear (DAD) and quadratic (ELSD) (correlation coefficients > 0.995).<sup>[22]</sup> The calibration curve equation, the limit of detection (LOD), and correlation coefficient ( $R^2$ ) of the individual FA standards are provided in Table S2, Supporting information. After FA quantification, the ratios among the most abundant FA were calculated. The FA profiles of normal and cancer cell lines (VERO cells, undifferentiated Caco-2 cells, differentiated Caco-2 cells, and B16F10 cells) used for FA ratio profile comparison were previously obtained in similar experimental conditions as reported (Table S1, Supporting Information, and citations therein).

#### 2.5. Statistical Analysis

Data were expressed as a mean  $\pm$  standard deviation (SD). Evaluation of the statistical significance of differences was performed using Graph Pad INSTAT software (GraphPad Software, San Diego, CA, USA) Normal distribution of data was preliminarily assessed. Comparison of means (FA and FA ratios) between two groups (HeLa versus 3T3 cells) was assessed by Student's unpaired *t*-test with Welch's correction, which does not require the assumption of equal variance between populations. Values with  $p < 0.05$  were considered significant.

#### 2.6. Chemometrics

Cell FA data (expressed as % of total FA, g/100 g) and FA ratios (normalized to 100) were collected in the data matrix, where rows were the cell samples (observations) and columns were the FA/FA ratios concentrations (variables). The generated data matrix was imported into the SIMCA software (Version 16.0, Sartorius Stedim Biotech, Umea, Sweden) and submitted to unit

variance scaling before principal components analysis (PCA) was performed. The result of PCA analysis was depicted as a scores plot (observations plot) and loadings plot (variables plot). PCA is considered an unsupervised analysis as allows the exploration of the distribution of the sample without prior classification.<sup>[26]</sup> The PCA scores plot reveals any inherent clustering of groups of data, trends, or outliers, based purely on the closeness or similarity between the samples, while the PCA loadings plot describes the influence of the variables in the model. An important feature is that directions in the scores plot correspond to directions in the loadings plot, and vice versa.<sup>[28]</sup>

The following formula:<sup>[26]</sup>

$$d(P_A, P_B) = \sqrt{(x_B - x_A)^2 + (y_B - y_A)^2} \quad (1)$$

(where:  $P_B$  is the control HeLa cells and  $P_A$  the HeLa cells treated with a specific drug concentration;  $x_B$  is  $t[1]$  of control cells;  $x_A$  is  $t[1]$  of treated cells;  $y_B$  is  $t[2]$  of control cells;  $y_A$  is  $t[2]$  of treated cells) was used to calculate in the PCA plot for HeLa cell treatment with different drugs the distance between the score of control HeLa cells and the score of treated cells in the same experimental set.

### 3. Results

#### 3.1. FA Ratios as Biochemical Markers to Characterize and Differentiate Cells

In the first part of the study, twenty-six cell samples belonging to two different cell lines (cancer HeLa cells and normal 3T3 fibroblasts) were characterized and compared for their fatty acid (FA) and FA ratio profiles by a biochemical and chemometric approach to explore the potential role of FA ratios as biochemical markers to characterize and differentiate cells. HeLa cells (Figure 1A), a cell line derived from epithelioid cervix carcinoma, represent a cultured cancer cell model amply used to assess the lipid modulatory properties of anticancer extracts and compounds.<sup>[22–25,29]</sup> 3T3 mouse fibroblasts (Figure 1B) are considered an excellent model system to study the plasma membrane FA composition/modulation in normal cells.<sup>[5]</sup> For each cell line, four different experiments were performed, with different replicates in each experiment. Experimental sets were conducted under the same experimental conditions at different times over 2 years. Total lipids were extracted from 3T3 fibroblast and HeLa cell pellets, saponified and analyzed for FA composition; and then, the ratios between the main FA were calculated.

Figure 2A shows the representative chromatographic profile, obtained by HPLC-DAD/ELSD analysis, of unsaturated (DAD detection) and saturated (ELSD detection) FA measured in cancer HeLa cells. Values of FA (expressed as % of total FA) measured in HeLa cell samples from different experiments (Exp. A, Exp. B., Exp. C., and Exp. C; each stacked bar in the graph represents the total % FA profile of a single cell sample) are reported in Figure 2B. Slight differences in the FA amounts were observed among cell replicates within the same experimental set. Whereas more marked differences were evidenced in HeLa cell FA levels between different experimental sets; although, the application of standardized conditions for cell growth, cell extraction, and FA

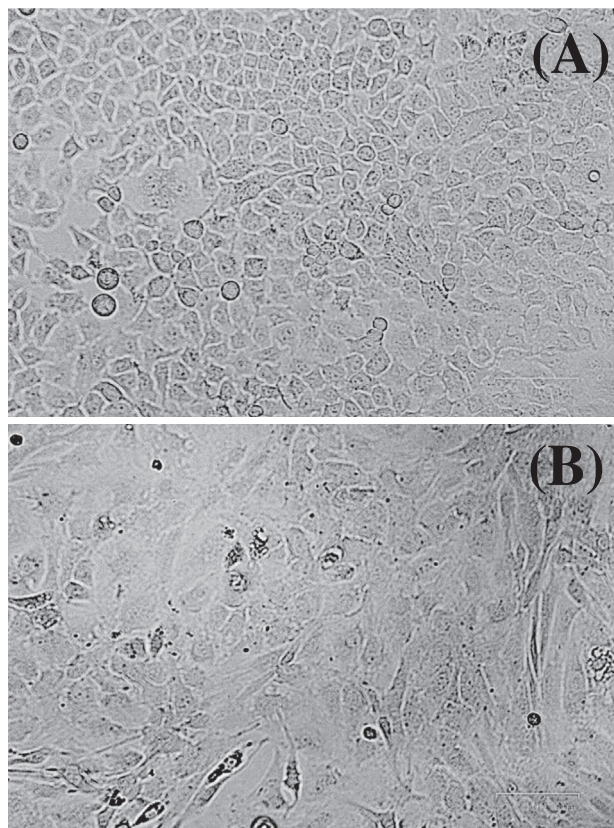


**Figure 1.** The panel shows representative images of A) phase contrast of cancer HeLa cells and B) 3T3 normal fibroblasts. Bar = 100  $\mu$ m.

analysis. Mean values and standard deviation (SD) of FA measured in HeLa cells from all experiments ( $n = 11$ ) expressed as % of total fatty acids and as  $\mu$ g per plate are reported in Figure 2C,D, respectively. HeLa cells showed a mean FA composition characterized by a high level of 18:1 isomers (mainly 18:1  $n-9$ ; 126.4  $\pm$  30.9  $\mu$ g per plate, 40% of total FA), 16:0 (70.7  $\pm$  26.2  $\mu$ g per plate, 22%), stearic acid 18:0 (38.6  $\pm$  22.2  $\mu$ g per plate, 11%), and palmitoleic acid 16:1  $n-7$  (25.6  $\pm$  6.7  $\mu$ g per plate, 8%), while 20:4  $n-6$  (14.6  $\pm$  2.4  $\mu$ g per plate, 5%) represented the most abundant FA among polyunsaturated FA (PUFA), followed by docosahexaenoic acid 22:6  $n-3$  (8.8  $\pm$  1.4  $\mu$ g per plate, 3%).

The chromatographic profile and %FA values measured in 3T3 cell samples from different experiments (Exp. A. Exp. B. Exp. C. and Exp. C; each stacked bar in the graph represents the total % FA profile of a single cell sample) are reported in Figures 3A and 3B, respectively. Like HeLa cells, more marked differences were evidenced in cell FA levels between different experimental sets than between cell replicates within the same experimental set even though comparable experimental conditions were used. Figure 3C,D shows the total mean values (expressed as % of total fatty acids and as  $\mu$ g per plate, respectively)  $\pm$  SD of FA measured in 3T3 fibroblasts from all experiments ( $n = 15$ ). 3T3 fibroblasts showed a FA composition characterized by a high level of oleic acid 18:1  $n-9$  (18.3  $\pm$  5.3  $\mu$ g per plate, 26% of total FA), palmitic acid 16:0 (12.7  $\pm$  2.6  $\mu$ g per plate, 18%), stearic acid 18:0 (12.1  $\pm$  2.5  $\mu$ g per plate, 17%), and palmitoleic acid 16:1  $n-7$  (1.9  $\pm$  0.9  $\mu$ g

per plate, 2%), while linoleic acid 18:2  $n-6$  (6.8  $\pm$  1.5  $\mu$ g per plate, 10%) and arachidonic acid 20:4  $n-6$  (6.5  $\pm$  1.6  $\mu$ g per plate, 9%) represented the most abundant FA among polyunsaturated FA (PUFA), followed by docosahexaenoic acid 22:6  $n-3$  (4.1  $\pm$  1.0  $\mu$ g per plate, 6%). The two cell lines showed differences in terms of FA profile, though similar growth conditions. Cancer HeLa cells were characterized by a higher % amount of SFA and PUFA and a lower % amount of MUFA than 3T3 fibroblasts. Significant differences were observed in the % level of 18:1  $n-9$  ( $p < 0.0001$ ), 16:1  $n-7$  ( $p < 0.0001$ ), 18:2  $n-6$  ( $p < 0.0001$ ), 20:3  $n-9$  ( $p < 0.0001$ ), 20:4  $n-6$  ( $p < 0.0001$ ), and 22:6  $n-3$  ( $p < 0.0001$ ) between the two cell lines.

However, 18:1  $n-9$ , 16:0, 18:0, 16:1  $n-7$ , 18:2  $n-6$ , 20:4  $n-6$ , and 22:6  $n-3$  emerged as the most abundant FA in both cell lines. Therefore, we decided to calculate the ratios between these main FA in order to explore the use of FA ratios as cell-specific dimensionless parameters for cell characterization and observe their reproducibility across intra-laboratory conditions. Figure 4 shows the values of the ratios between the main FA measured in each sample of HeLa cells (Figure 4A) and 3T3 fibroblasts (Figure 4B) from different experiments together with the mean values  $\pm$  SD of FA ratios obtained from all experiments. For each cell line, differences were observed in the total FA ratios between different experiments, indicative of differences in FA composition due to the experimental variability. The two cell lines showed a specific profile of FA ratios. High ratio values were measured for 18:1  $n-9$ /22:6  $n-3$  ( $p < 0.0001$  versus 3T3 cells), 18:1  $n-9$ /18:2  $n-6$  ( $p < 0.0001$ ), 18:1  $n-9$ /20:4  $n-6$  ( $p < 0.0001$ ), and 16:0/18:2  $n-6$  ( $p < 0.0001$ ) in cancer HeLa cells, while 3T3 fibroblasts were characterized by high values of the 18:1  $n-9$ /16:1  $n-7$  ( $p < 0.0001$ ), 16:0/16:1  $n-7$  ( $p < 0.0001$ ), and 18:1  $n-9$ /22:6  $n-3$  ratios.

Then, we used a chemometric approach to compare the FA and FA ratio profiles of cancer HeLa cells and 3T3 fibroblasts. The principal component analysis (PCA) of the FA and FA ratios profile of HeLa and 3T3 cell samples was performed to have a comparative holistic picture of the two cell lines and therefore a clear indication of the role of FA ratios as alternative set data for cell type characterization. PCA plot shows clusters of samples based on their similarity.<sup>[26]</sup> Figure 5 shows the PCA scores plot (Figure 5A) and loadings plot (Figure 5B) of FA data (expressed as % of total FA) measured in cancer HeLa cells ( $n = 11$ ) and 3T3 fibroblasts ( $n = 15$ ) obtained from different experiments as reported in Figures 2B and 3B, respectively. Results of FA cell compositions are depicted as PCA scores plot where the distribution of cell samples (Figure 5A) and the variables along the first two principal components (PC) (Figure 5B) are displayed. Cell samples with a similar FA profile lie in a single class in the PCA scores plot.<sup>[26]</sup> The FA contribution to the sample clustering can be estimated considering that the position of a sample in a specific direction in the scores plot is influenced by the FA lying in the same direction in the corresponding loadings plot. Cell samples situated in the same direction as the FA indicated in the loading plot, are high in these variables and are low in the variables situated in the opposite space of PCA along PC1.<sup>[26]</sup> Hence, the scores plot indicated that cell samples clustered according to their specific FA composition. A clear separation was observed in the PCA scores plot between HeLa and 3T3 cell samples, which clustered in two different positions of the plot, indicating a different FA composition. In detail, all HeLa cell samples clustered

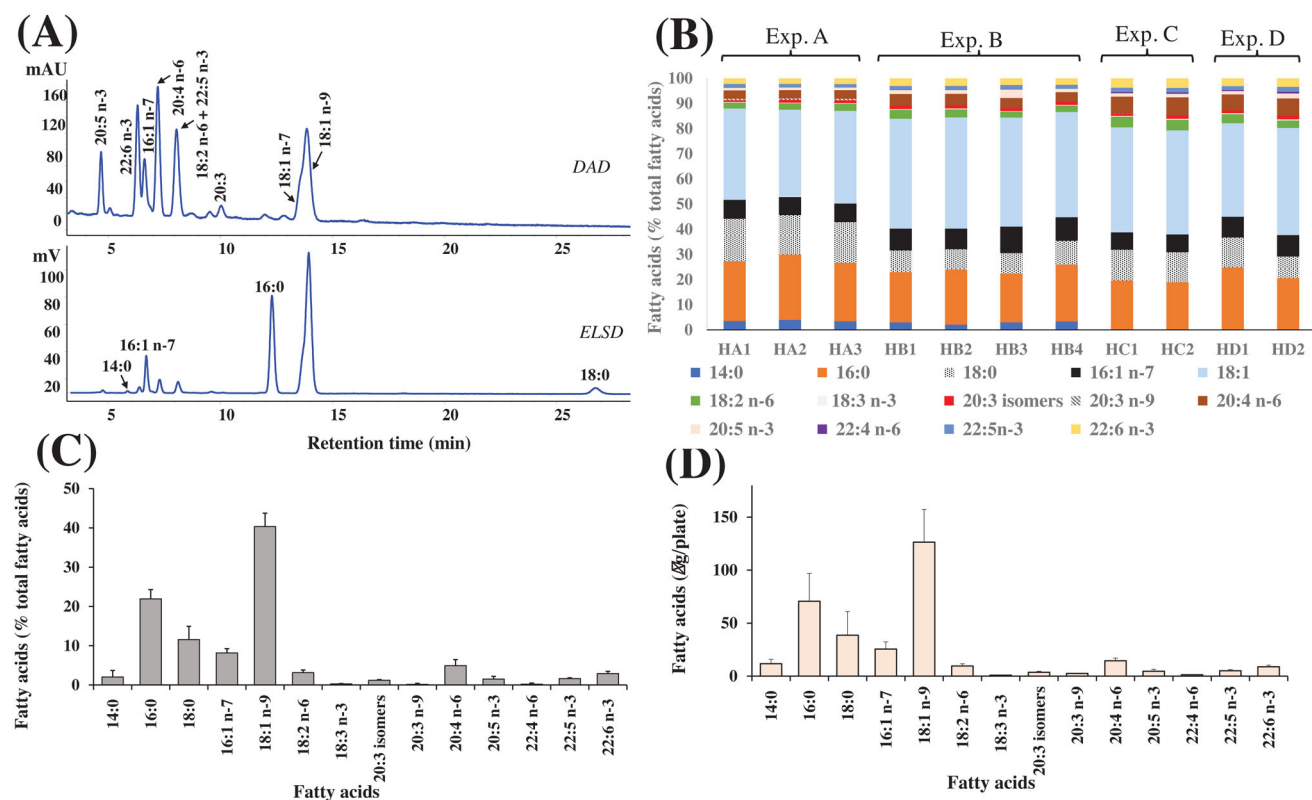


**Figure 2.** A) Chromatographic profile, obtained by HPLC-DAD/ELSD analysis, of unsaturated (DAD) and saturated (ELSD) FA measured in a sample of cancer HeLa cells. B) Each stacked bar represents total FA values (expressed as % of total fatty acids) measured in each HeLa cell sample from different experiments (Exp. A, Exp. B, Exp. C, and Exp. D); different replicates were performed in each experiment. Mean values ( $n = 11$ ) and standard deviation (SD) of FA measured in control HeLa cells from all experiments, expressed as C) % of total FA and D) as  $\mu\text{g}$  per plate.

to negative values along  $t[1]$  in the scores plot and were mainly characterized by 16:0, MUFA (18:1  $n-9$  and 16:1  $n-7$ ), and 20:5  $n-3$ , 22:5  $n-3$ , and 18:3  $n-3$ . 3T3 cell samples clustered to positive values along  $t[1]$ , differing from HeLa cell for the high amounts of 20:3  $n-9$ , 22:4  $n-6$ , 18:2  $n-6$ , 22:6  $n-3$ , 20:4  $n-6$ , and SFA 14:0 and 18:0. For each cell type, the observed distance among samples was an indication of some differences in the amounts of specific FA, ascribable to the sample experimental variability. Then, a PCA was performed using the values of the ratios among the main FA (normalized values reported in Figure 4A,B) measured in each sample of cancer HeLa cells ( $n = 11$ ) and 3T3 fibroblasts ( $n = 15$ ) from the different experiments. PCA scores plot and loadings plot of FA ratios data (normalized to 100) measured in HeLa and 3T3 cells are reported in Figures 5C and 5D, respectively. As observed in the PCA of FA values, samples of the two cell lines clustered in two different positions of the plot in relation to their specific FA ratio profile. Cancer HeLa cell samples clustered to negative values along  $t[1]$  and were mainly characterized by 16:0/18:2  $n-6$ , 18:1  $n-9$ /20:4  $n-6$ , and 18:1  $n-9$ /22:6  $n-3$ , while 3T3 fibroblasts were characterized by 20:4  $n-6$ /22:6  $n-3$  and 18:1  $n-9$ /16:1  $n-7$  ratios. PCA performed on both FA and FA ratio data clearly showed a marked separation between the two cell lines, and the clustering of cell samples based on the cell type was similar in the two PCA plots, qualifying the FA ratio profile as a cell-specific fingerprint, characterized by a good reproducibility across intra-laboratory conditions.

### 3.2. FA Ratios as Biochemical Markers to Compare Different Drug Treatments in Cancer Cells

Then, the same biochemical and chemometric approach was applied to explore the use of cell FA ratios as parameters to compare the effect on FA metabolism of different treatments in the same cancer cell line and validate their potential as biomarkers for quantitative purposes. Cancer HeLa cells were incubated with several anticancer drugs in different experimental sets conducted at different times, as previously reported: zerumbone (Treatment A; 10, 50, and 100  $\mu\text{M}$ ),<sup>[22]</sup> eupatilin (Treatment B; 10, 25, and 50  $\mu\text{M}$ ),<sup>[23]</sup> artemetin (Treatment C; 10, 25 and 50  $\mu\text{M}$ ),<sup>[24]</sup> and its derivatives 8-prenyl artemetin and 5-O-prenyl artemetin (Treatment D, 25  $\mu\text{M}$ ).<sup>[25]</sup> Total lipids were extracted from control HeLa cells and cells subjected to different treatments, saponified, analyzed for FA composition,<sup>[22–25]</sup> and ratios between the main cell FA (18:1  $n-9$ , 16:0, 18:0, 16:1  $n-7$ , 18:2  $n-6$ , 20:4  $n-6$ , and 22:6  $n-3$ ) were calculated. **Figure 6** shows mean values  $\pm$  SD of FA (expressed as % of total FA) (Figure 6A) and FA ratios (expressed as the sum of ratios between the main FA) (Figure 6B) measured in control cancer HeLa cells (CA, CB, CC, and CD) and cells treated with anticancer compounds in the different experimental sets. The chemical structures of the tested compounds are also reported in Figure 6A. All tested compounds, at non-cytotoxic concentrations, induced modulation of the HeLa cell FA profile<sup>[22–25]</sup> and consequently affected the FA ratio profile versus

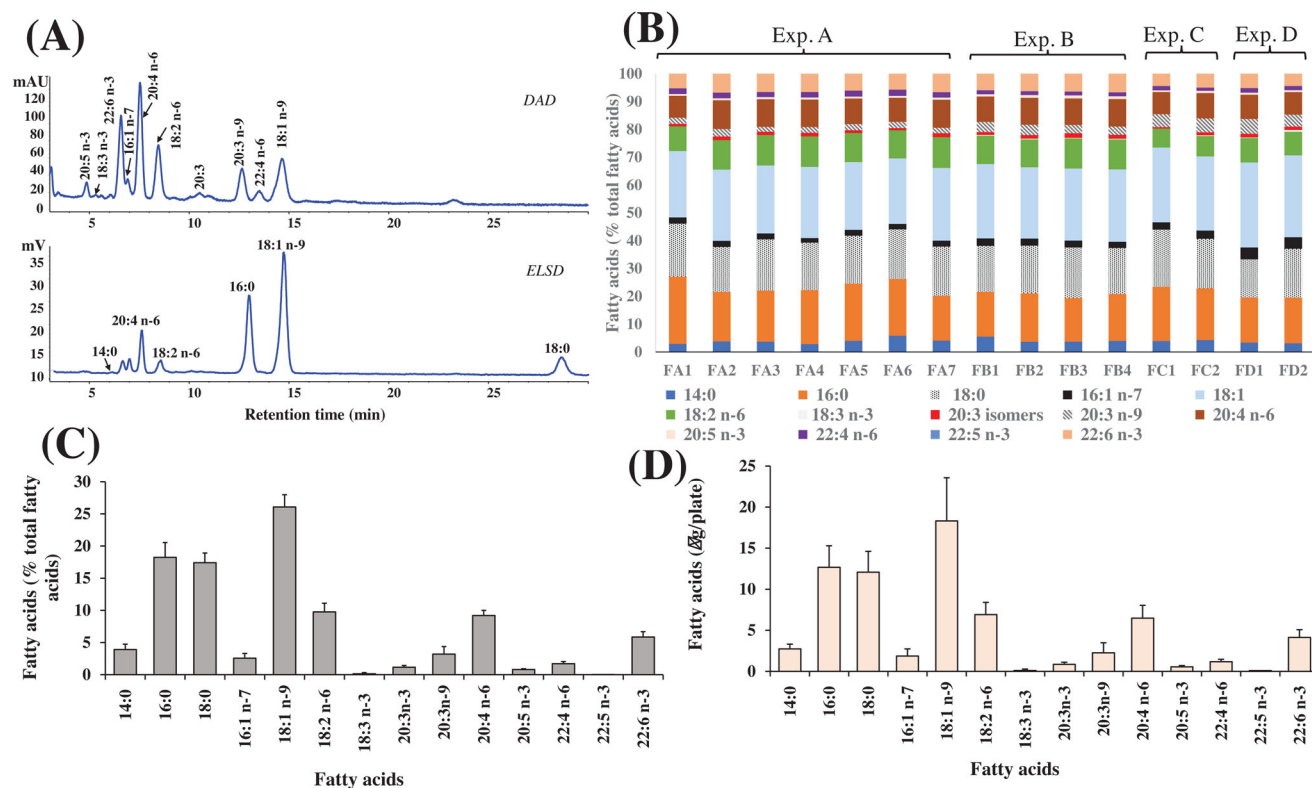


**Figure 3.** A) Chromatographic profile, obtained by HPLC-DAD/ELSD analysis, of unsaturated (DAD) and saturated (ELSD) FA measured in a sample of murine 3T3 fibroblasts. B) Each stacked bar represents total FA values (expressed as % of total FA) measured in each 3T3 cell sample from different experiments (Exp. A, Exp. B, Exp. C, and Exp. D); different replicates were performed in each experiment. Mean values ( $n = 15$ ) and standard deviation (SD) of FA measured in control HeLa cells from all experiments, expressed as C) % of total FA and as D)  $\mu\text{g}$  per plate.

the corresponding control cells. The incubation of cancer HeLa cells with zerumbone<sup>[22]</sup> induced marked changes in the FA profile versus untreated control cells from the dose of  $50 \mu\text{M}$ , with a marked decrease in the % cell level of 18:1 *n*-9 and 16:0, and an increase in the % amount of 18:0. HeLa cells incubated with eupatilin<sup>[23]</sup> showed a reduction in the % levels of 16:0 and 18:1 *n*-9 at all tested doses together with a % increase in the level of 18:0 from the dose of  $10 \mu\text{M}$ . The incubation of cancer HeLa cells with artemetin<sup>[24]</sup> induced a dose-response decrease in the cell level of 18:1 *n*-9, 16:1 *n*-7, and 16:0. Differently, cell treatment with both prenylated artemetin derivatives<sup>[25]</sup> induced at the dose of  $25 \mu\text{M}$  marked reduction in the levels of 18:1 *n*-9 and 16:1 *n*-7, together with a % increase in the level of 16:0, 18:0, and several PUFA (20:3, 22:5 *n*-3, 22:4 *n*-6, and 22:6 *n*-3). A marked dose-dependent decrease in the total values of the ratios between the main FA was observed in HeLa cells treated with different anticancer compounds (Figure 6B) versus control cells, especially in the values of 18:1 *n*-9/22:6 *n*-3, 18:1 *n*-9/18:2 *n*-6, 18:1 *n*-9/20:4 *n*-6, 16:0/18:2 *n*-6, and 16:0/22:6 *n*-6, due to the changes induced in the FA acid metabolism.<sup>[22–25]</sup>

Then, PCA was separately applied to FA and FA ratio data measured in HeLa cells treated with anticancer compounds. **Figure 7** shows the PCA scores plot and loadings plot of mean values of FA (expressed as % of total FA) (Figure 7A,B) and FA ratios data (normalized to 100) (Figure 7C,D) measured in control cancer HeLa cells (CA, CB, CC, and CD) and cells treated

with several anticancer compounds in the four experimental sets (Treatment A, B, C, D). PCA performed on FA and FA ratio data showed similar clustering of HeLa cell samples based on the cell treatment and dose of treatment. To quantify the differences between treatments, and for each treatment between the different tested doses, lines were traced in the PCA score plots (Figure 7A,C) to indicate the distances between the values of treated cells and their respective control cells. The graphical distances in the PCA plots between the score of control cells and the score of their respective treated cells were calculated according to the formula reported in subparagraph 2.5. **Table 1** shows the scores values  $t[1]$  and  $t[2]$  and graphical distances calculated in the PCA plots (reported in Figure 7A,C). Distance values calculated in the PCA scores plot obtained with FA data ranged from 0.77 to 4.85. In general, for the treatment with zerumbone, eupatilin, and artemetin, our data evidenced a dose-dependent increase in the distance values versus control cells. A marked modulatory effect on the FA profile corresponded to a greater distance. The highest distance values were measured for cells treated with prenylated artemetin derivatives at the dose of  $25 \mu\text{M}$ , which induced a marked change in the FA profile. Scores values  $t[1]$  and  $t[2]$  and graphical distances (values ranging from 0.56 to 3.73) calculated in the PCA plot of FA ratio data were quite similar to those measured in the PCA plot obtained with FA data. Moreover, a high positive correlation coefficient ( $r = 0.9543$ ) was determined between graphical distances measured

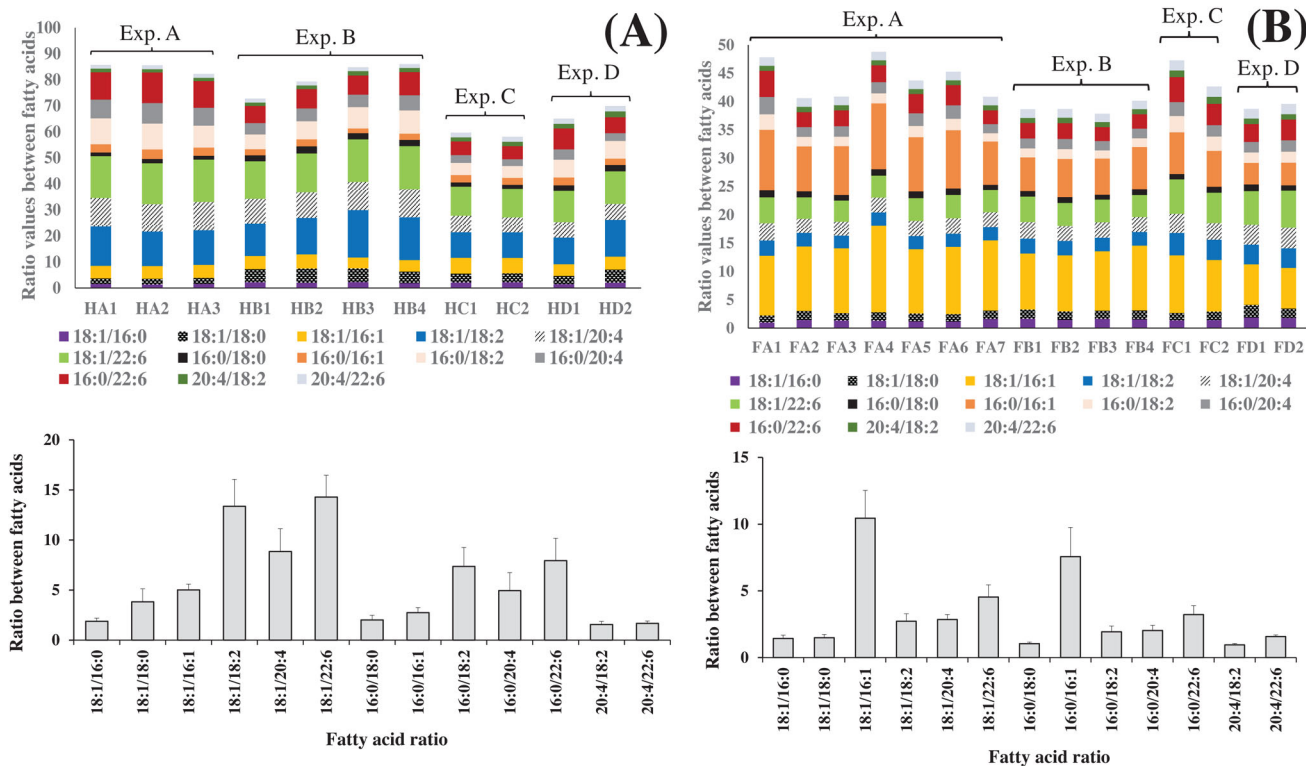


**Figure 4.** Values of the ratios among the main FA measured in each cell sample from different experiments (Exp. A, Exp. B, Exp. C, and Exp. D with different replicates in each experiment) and mean values and standard deviation (SD) of FA ratios from all experiments determined A) in control HeLa cells ( $n = 11$ ) and B) murine 3T3 fibroblasts ( $n = 15$ ). Each stacked bar chart represents the sum of FA ratios determined in each cell sample.

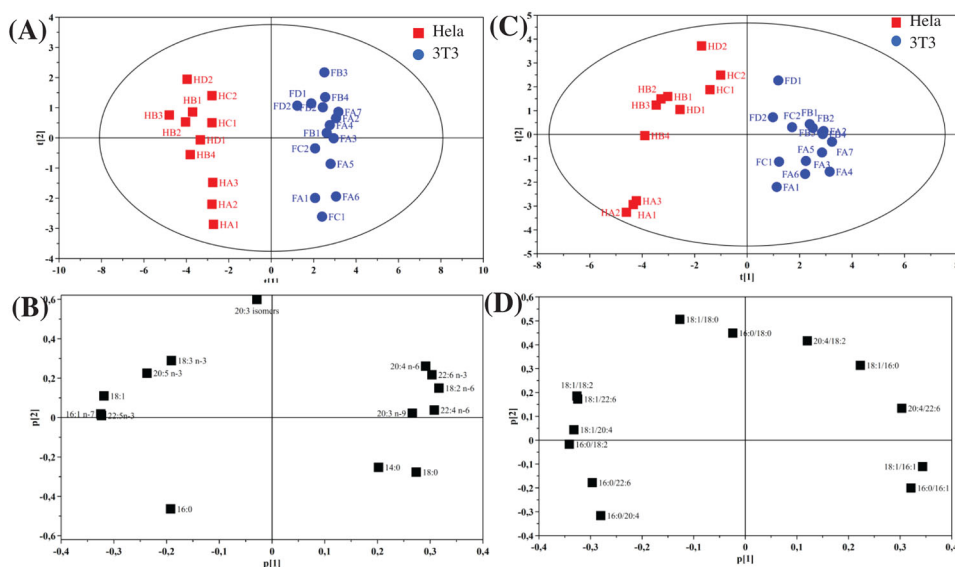


**Figure 5.** A) PCA scores plot and B) loadings plot of FA data (expressed as % of total FA), measured in control cancer HeLa cells ( $n = 11$ ) and murine 3T3 fibroblasts ( $n = 15$ ) obtained from different experiments as reported in Figures 1B and 2B, respectively. C) PCA scores plot and D) loadings plot of FA ratios data (normalized to 100) measured in HeLa and 3T3 cells as reported in Figure 4A,B, respectively. For each PCA model (A and C), the first two PC explain 80% and 86% of the total variance, respectively.

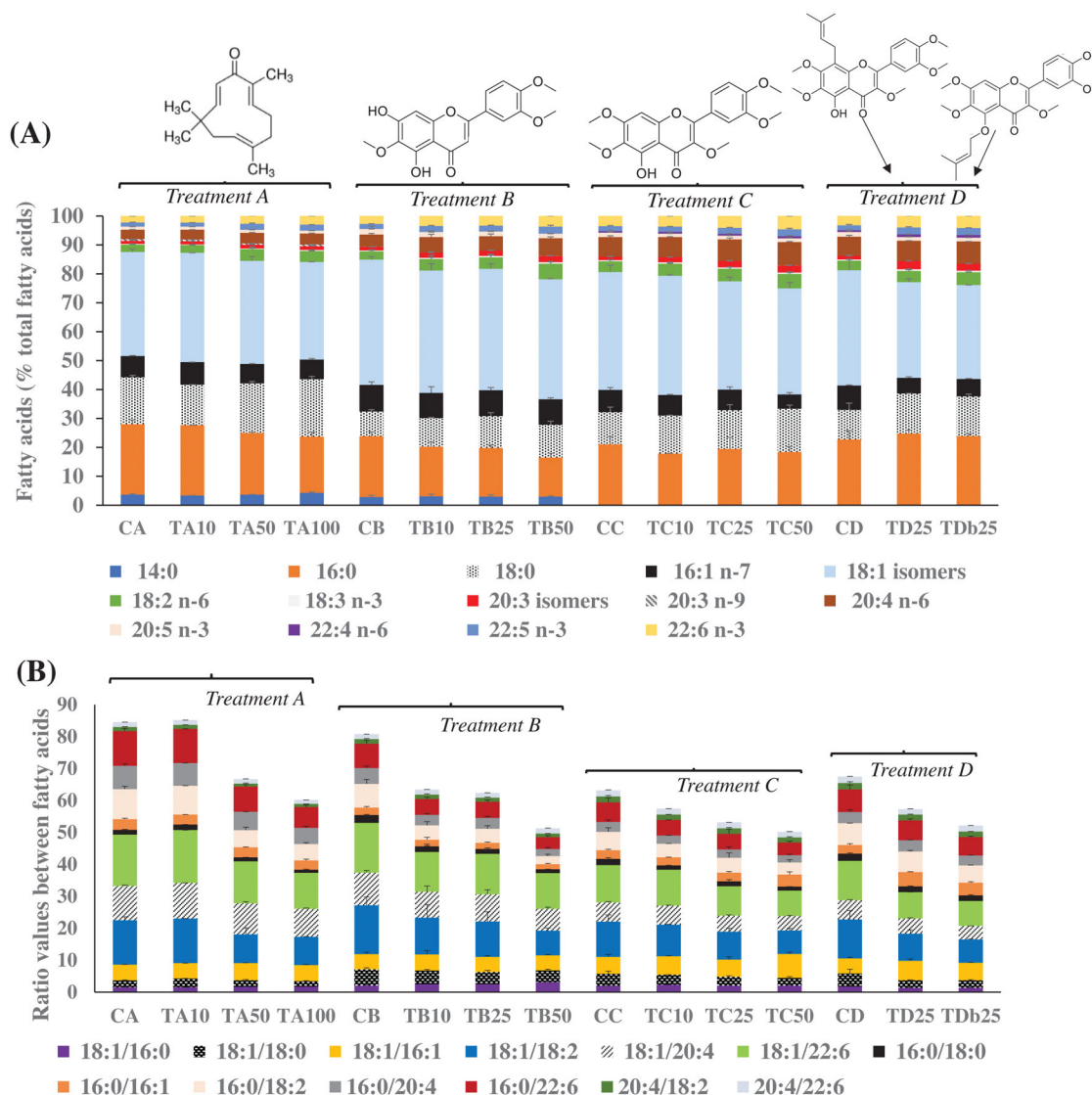


**Figure 6.** A) Mean values and standard deviation (SD) of FA (expressed as % of total FA)<sup>[22–25]</sup> and B) FA ratios measured in control cancer HeLa cells (CA, CB, CC, and CD) and cells treated with several anticancer compounds in four different experimental sets: Treatment A: zerumbone 10, 50, and 100  $\mu\text{M}$  (TA10, TA50, and TA100); Treatment B: eupatilin 10, 25, and 50  $\mu\text{M}$  (TB10, TB25, and TB50); Treatment C: artemetin 10, 25, and 50  $\mu\text{M}$  (TC10, TC25, and TC50); Treatment D: 8-prenyl artemetin 25  $\mu\text{M}$  (TD25) and 5-*O*-prenyl artemetin 25  $\mu\text{M}$  (TDb25).

for all treatments in the FA and FA ratio data plots, indicating the interchangeability of the two data series. Our results qualified the FA ratio profile as a cell-specific data set, useful to compare, across intra-laboratory conditions, the modulatory effect on lipid metabolism of different drug treatments in cultured cells.

### 3.3. FA Ratios as Biochemical Markers to Discriminate Between Normal and Tumoral Cells

PCA scores plot (Figure 5C) obtained for HeLa and 3T3 cells substantiated FA ratios as suitable parameters to distinguish different cell lines. Therefore, a small set of FA ratios was selected, based on analytical considerations, and calculated for other cell lines previously cultured/analyzed in our laboratories. Then,

PCA was applied to selected FA ratios from different cell lines to explore FA ratios as potential analytical markers for differentiating between normal and cancer cells.

The FA ratios were selected based on criteria such as the position in the PCA plot along  $t[1]$  and the easy analytical determination of the corresponding FA. The position along  $t[1]$  in the PCA plot performed on FA ratios (Figure 5C) indicated high values of 16:0/18:2 *n*-6, 18:1 *n*-9/20:4 *n*-6, and 18:1 *n*-9/22:6 *n*-3 in cancer HeLa cells, while 3T3 fibroblasts were mainly characterized by 20:4 *n*-6/22:6 *n*-3 and 18:1 *n*-9/16:1 *n*-7 ratios. In our chromatographic separation conditions, oleic acid 18:1 *n*-9, palmitic acid 16:1 *n*-7, arachidonic acid 20:4 *n*-6, and docosahexaenoic acid 22:6 *n*-3 were characterized by a selective and easy detection for the high intensity of the signal and/or high peak purity, while 18:2 *n*-6 quantification was complicated by the partial co-elution with

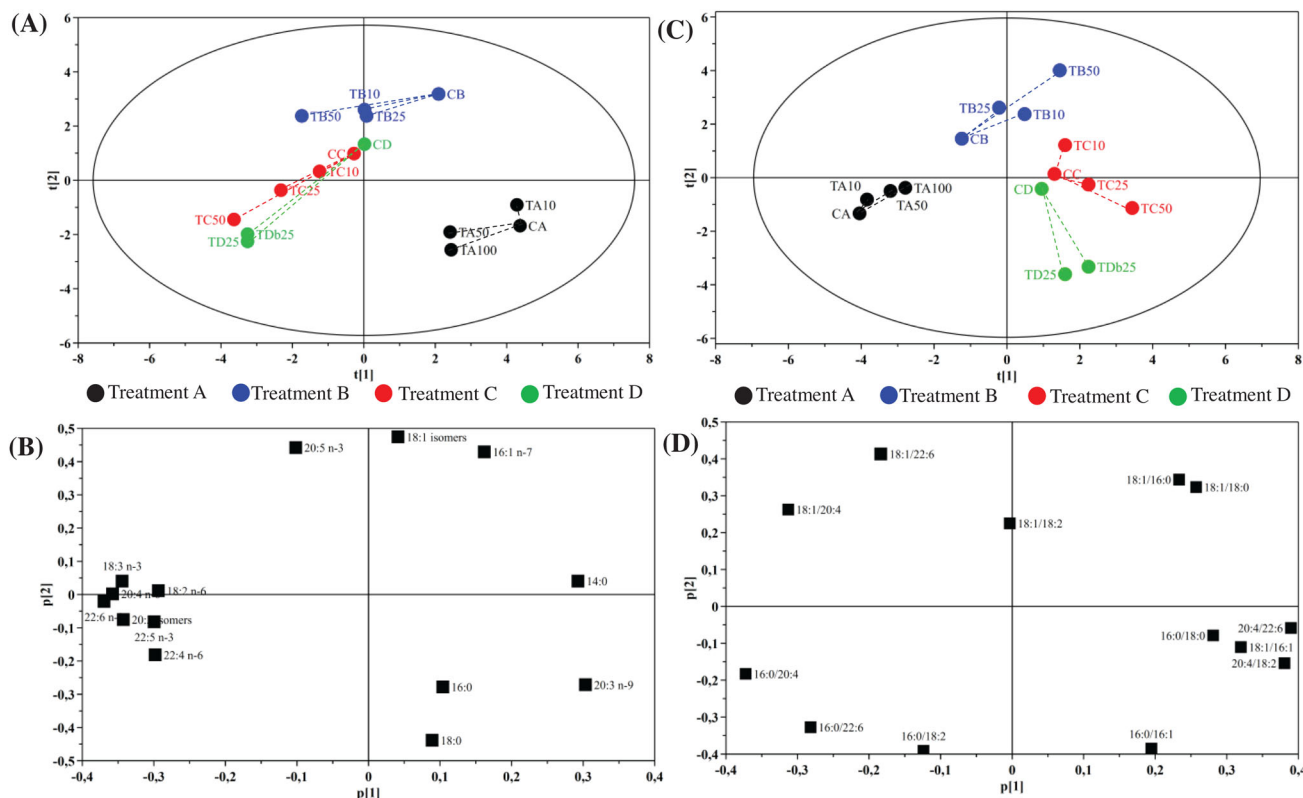


**Figure 7.** A) PCA scores plot and B) loadings plot of mean values of FA (expressed as % of total FA)<sup>[22–25]</sup> measured in control cancer HeLa cells (CA, CB, CC, and CD) and cells treated with several anticancer compounds in four different experimental sets: Treatment A: zerumbone 10, 50, and 100  $\mu\text{M}$  (TA10, TA50, and TA100); Treatment B: eupatilin 10, 25, and 50  $\mu\text{M}$  (TB10, TB25, and TB50); Treatment C: artemetin 10, 25, and 50  $\mu\text{M}$  (TC10, TC25, and TC50); Treatment D: 8-prenyl artemetin 25  $\mu\text{M}$  (TD25) and 5-O-prenyl artemetin 25  $\mu\text{M}$  (TD25). C) PCA scores plot and D) loadings plot of mean values of FA ratios, normalized to 100, measured in control and treated HeLa cells of the four treatments. For each set of experiments, the lines traced in the PCA score plot indicate the distances between the values of control cells and their respective treated cells. For each PCA model, the first two PC explain 80% of the total variance.

22:5 *n-3*, as previously reported.<sup>[22]</sup> Therefore, 18:1 *n-9*/20:4 *n-6*, 18:1 *n-9*/22:6 *n-3*, 18:1 *n-9*/16:1 *n-7*, and 20:4 *n-6*/22:6 *n-3* were selected for HeLa and 3T3 cells. These FA ratio values were calculated for other normal (VERO cells) and cancer (undifferentiated and differentiated Caco-2 cells, and B16F10 cells) cell lines using FA data previously obtained from different experimental sets performed in our laboratories in similar experimental conditions (Table S1, Supporting Information, and citations therein). Unsaturated FA profiles (expressed as  $\mu\text{g}/\text{plate}$ ) measured in VERO cells, undifferentiated Caco-2 cells, differentiated Caco-2 cells, and B16F10 cells by HPLC-DAD analysis are reported in Figure S1, Supporting Information. Values of selected FA ratios 18:1 *n-9*/16:1 *n-7*, 18:1 *n-9*/20:4 *n-6*, 18:1 *n-9*/22:6 *n-3*, and 20:4 *n-6*/22:6 *n-3* calculated for VERO cells, undifferentiated/differentiated Caco-2 cells, and B16F10 cells, in comparison with those obtained for 3T3 and HeLa cells, are depicted in **Figure 8A**. Cancer undifferentiated/differentiated Caco-2 cells, HeLa cells, and B16F10 cells were very similar in terms of FA ratio profile unless some differences were observed in the absolute values of selected FA ratios. Interestingly, 3T3 and VERO fibroblasts differed from other cells for their FA ratios. In **Figure 8B**, the PCA scores plot built using the values of the selected FA ratios show how the single component  $t[1]$  can distinguish between normal fibroblasts (positive

values of  $t[1]$ ) and cancer cells (negative values of  $t[1]$ ). Our results substantiated FA ratios as a suitable metabolic parameter to discriminate between normal and tumoral cells across intra-laboratory conditions.

#### 4. Discussion

FA, as structural components of membranes and inflammation/anti-inflammatory mediators, display regulatory effects on cell homeostasis and physiological functions, and represent indispensable substrates for  $\beta$ -oxidation and ATP production.<sup>[4,5,30]</sup> Cell membrane FA composition is tightly regulated and changes in cell FA components can modify the structure of the lipid membrane, altering its microdomain organization and other physical properties, and inducing changes in cell signaling.<sup>[30,31]</sup> Cancer cells are characterized by a deregulation of FA metabolism, showing high rates of de novo lipid synthesis and exogenous FA uptake.<sup>[1,3,7–9]</sup> Therefore, the FA profile has been considered a homeostatic and metabolic biomarker for evaluating differences in FA metabolism in normal and cancer cells.<sup>[4,5,10,11]</sup> In vitro cell models offer a unique opportunity for conducting studies on differences in FA metabolism between normal and cancer cells and the drug-modulatory effect

**Table 1.** Scores values  $t[1]$  and  $t[2]$  and calculated distances (between the values of control cells and their respective treated cells) in the PCA plots (reported in Figure 7A,C) of mean values of FA (expressed as % of total fatty acids) and FA ratios, normalized to 100, measured in control cancer HeLa cells (CA, CB, CC, and CD) and cells treated with several anticancer compounds in four different experimental sets: Treatment A, zerumbone 10, 50, and 100  $\mu\text{M}$  (TA10, TA50, and TA100); Treatment B, eupatilin 10, 25, and 50  $\mu\text{M}$  (TB10, TB25, and TB50); Treatment C, artemetin 10, 25, and 50  $\mu\text{M}$  (TC10, TC25, and TC50); Treatment D, 8-prenyl artemetin 25  $\mu\text{M}$  (TD25) and 5-*O*-prenyl artemetin 25  $\mu\text{M}$  (TDb25).

Treatment	Primary ID	$t[1]$	$t[2]$	Distance
%Fatty acids (normalized)				
A	CA	4.3826	-1.6793	—
A	TA10	4.2818	-0.9102	0.7757
A	TA50	2.4168	-1.8912	1.9772
A	TA100	2.4427	-2.5698	2.1345
B	CB	4.3826	-1.6793	—
B	TB10	4.2818	-0.9102	2.1730
B	TB25	2.4168	-1.8912	2.1987
B	TB50	2.4427	-2.5698	3.9286
C	CC	4.3826	-1.6793	—
C	TC10	4.2818	-0.9102	1.1662
C	TC25	2.4168	-1.8912	2.4574
C	TC50	2.4427	-2.5698	4.1476
D	CD	4.3826	-1.6793	—
D	TD25	4.2818	-0.9102	4.8490
D	TDb25	2.4168	-1.8912	4.6453
Fatty acid ratios (normalized)				
A	CA	-4.0454	-1.3425	—
A	TA10	-3.8362	-0.8251	0.5581
A	TA50	-3.2022	-0.4940	1.1962
A	TA100	-2.7827	-0.3867	1.5837
B	CB	-1.2322	1.4414	—
B	TB10	0.4931	2.3665	1.9577
B	TB25	-0.2291	2.5999	1.5325
B	TB50	1.4608	4.0275	3.7336
C	CC	1.3145	0.1389	—
C	TC10	1.5999	1.2185	1.1166
C	TC25	2.2259	-0.2696	0.9989
C	TC50	3.4446	-1.1184	2.4735
D	CD	0.9592	-0.4058	—
D	TD25	1.6023	-3.6130	3.2711
D	TDb25	2.2276	-3.3374	3.1943

on lipid pathways.<sup>[5,17,22,29]</sup> Unfortunately, the reproducibility, reliability, and variability of the cell FA data across independent laboratories and intra-laboratory conditions depend on several specific factors related to cell culture conditions (cell handling, number of cell passages, cell consumable usage, cell growth phase),<sup>[16–18]</sup> lipid extraction procedure (solvent and condition used for extraction, extraction yield),<sup>[2]</sup> derivatization procedure (derivatization reagent and conditions, process yield),<sup>[2]</sup> and the limit of detection of the specific analytical technique used for FA identification/quantification.<sup>[2,19]</sup> Recent studies have

proposed FA ratios as a suitable way to efficiently replace the original FA data set for chemometric analysis.<sup>[19]</sup> FA ratios are believed to have sub-compositional coherence because the ratio between two specific FA remains the same whatever other FA are included, with or without normalization.<sup>[19]</sup> Moreover, the ratio between two FA is a dimensionless quantity.<sup>[19]</sup>

In this study, we explored the potential use of the FA ratio profile as a reproducible data set for the characterization/comparison of cells and the quantification/comparison of the modulatory effects on FA metabolism of different drug treatments in cell culture. In the first part of the study, cancer HeLa cells and normal 3T3 fibroblasts, from various experimental sets, were characterized for their FA profile and FA ratios. Even though experimental variability was observed among samples, PCA performed on FA ratio data clearly showed a marked separation between the two cell lines, and the clustering of cell samples concerning the cell type was like that observed in the PCA plot performed on the full FA data set. Previous studies used FA ratio analysis to discriminate trophic markers in marine pelagic organisms<sup>[19]</sup> and identify changes in competent meroplanktonic larvae sampled over different supply events.<sup>[32]</sup>

In our experimental conditions, from PCA plot and analytical considerations, a small set of FA ratios (18:1 *n*-9/16:1 *n*-7, 18:1 *n*-9/20:4 *n*-6, 18:1 *n*-9/22:6 *n*-3, and 20:4 *n*-6/22:6 *n*-3) emerged as the most representative to characterize/differentiate cancer HeLa cells and normal 3T3 fibroblasts. HeLa cells showed a higher % amount of 18:1 *n*-9 and 16:1 *n*-7 and lower % values of 20:4 *n*-6, and 22:6 *n*-3 than 3T3 fibroblasts. Therefore, higher values of 18:1 *n*-9/20:4 *n*-6 and 18:1 *n*-9/22:6 *n*-3 and lower values of 18:1 *n*-9/16:1 *n*-7 were determined in HeLa cells versus 3T3 cells. Oleic (18:1 *n*-9), palmitoleic (16:1 *n*-7) arachidonic (20:4 *n*-6), and docosahexaenoic (22:6 *n*-3) acids are important components of membrane lipids in normal and cancer cells and have crucial roles in biophysical, biochemical, and signaling processes.<sup>[4,29,33–35]</sup> Oleic and palmitoleic acids represent the main MUFA generally measured in cell cultures.<sup>[22,33]</sup> Stearoyl-CoA desaturase (SCD) catalyzes the introduction of the first double bond in the *cis*- $\Delta$ -9 position of several saturated fatty acyl-CoAs (mainly palmitoyl-CoA and stearoyl-CoA).<sup>[1,7,36,37]</sup> The major products of SCD, palmitoleic acid, and oleic acid, provide key substrates for the generation of complex lipids such as phospholipids, triglycerides, and cholesterol esters.<sup>[9]</sup> Several studies have reported that SCD is significantly increased in tumours, and SCD-mediated desaturation of FA may represent an important step for cancer cell survival.<sup>[36]</sup> Cancer cells often require *de novo* synthesis of unsaturated FA to generate membranes and maintain their fluidity.<sup>[37]</sup> An elevated synthesis of monounsaturated FA (MUFA), mainly oleic acids 18:1 *n*-9, has been measured in lung cancer<sup>[3]</sup> and colorectal cancerous tissue.<sup>[38]</sup> The predominant *n*-6 fatty acid for a broad range of cultured cell lines and natural cells is arachidonic,<sup>[29,33]</sup> which serves as the main precursor of several eicosanoid species (prostaglandins, thromboxanes, and leukotrienes), important regulators of cellular functions with inflammatory, atherogenic, and prothrombotic effects.<sup>[3,7,34]</sup> Specifically, enhanced metabolism of arachidonic acid to arachidonyl-CoA, which can be used as a substrate for cyclo-oxygenase 2 (COX2) for prostaglandin synthesis, has been observed in cancer cells.<sup>[3]</sup> Docosahexaenoic acid 22:6 *n*-3 is the most abundant PUFA of the *n*-3 series in cultured cells<sup>[29,33]</sup>

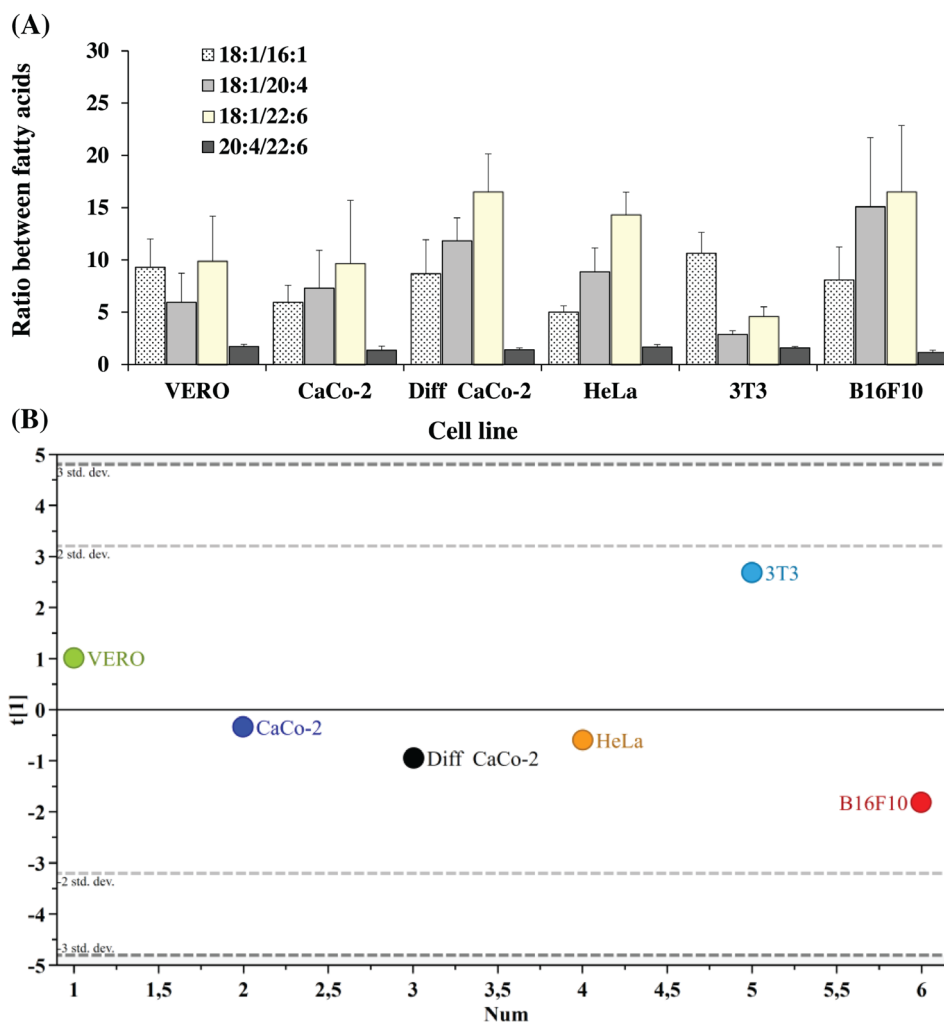


**Figure 8.** A) Mean values and standard deviation (SD) of FA ratios 18:1 *n*-9/16:1 *n*-7, 18:1 *n*-9/20:4 *n*-6, 18:1 *n*-9/22:6 *n*-3, and 20:4 *n*-6/22:6 *n*-3 measured in VERO cells (*n* = 39), 3T3 fibroblasts (*n* = 15) (normal cells) and CaCo-2 cells (*n* = 24), differentiated CaCo-2 cells (*n* = 33), HeLa cells (*n* = 11), and B16F10 cells (*n* = 6) (cancer cells). B) The PCA scores plot built using mean values of selected FA ratios. The PCA model was performed using a single component which explained 65% of the total variance.

and is the precursor of signaling molecules, that modulates membrane microdomain composition, receptor signaling, and gene expression.<sup>[35]</sup> An altered synthesis of 22:6 *n*-3 has been measured in lung cancer.<sup>[3]</sup> Then, we calculated the selected FA ratios (18:1 *n*-9/16:1 *n*-7, 18:1 *n*-9/20:4 *n*-6, 18:1 *n*-9/22:6 *n*-3, and 20:4 *n*-6/22:6 *n*-3) for other normal (VERO fibroblasts) and cancer (colon cancer undifferentiated and differentiated Caco-2 cells, and B16F10 murine melanoma cells) cell lines, previously grown and analyzed for FA profile under experimental conditions similar to those used for HeLa and 3T3 cells. Values of selected FA ratios measured in different cultured cell lines changed in relation to the specific cell FA metabolism, and the PCA scores plot performed on mean values of selected FA ratios showed a marked separation between normal and tumoral cells. Taking together our results substantiated FA ratios as a metabolic parameter suitable to characterize cells and discriminate between normal and tumoral cells across intra-laboratory conditions.

In cancer cells, changes in FA composition severely alter membrane fluidity and protein dynamics, affecting functional

and biophysical properties of cytoplasmic and organelle membranes, perturbing membrane lipid rafts, and inducing apoptotic pathways.<sup>[3,8,36]</sup> Several antitumor drugs (lipophilic or amphiphilic molecules) act through the membranes by changing the general lipid membrane structure and organization, by inhibiting the expression of lipogenic enzymes involved in FA metabolism such as SCD,<sup>[9,12–14]</sup> ATP-citrate lyase,<sup>[3,14]</sup> and FA synthase (FAS).<sup>[9,12–14]</sup> FAS is a multi-enzyme that catalyses de novo synthesis of palmitic acid, and many anticancer drugs are FAS inhibitors.<sup>[3,7,8,22]</sup> We previously demonstrated the ability of the antitumoral compounds zerumbone,<sup>[22]</sup> eupatilin,<sup>[23]</sup> artemetin,<sup>[24]</sup> and its derivatives 8-prenyl artemetin and 5-*O*-prenyl artemetin,<sup>[25]</sup> to reduce viability and modulate phospholipids and FA metabolism in HeLa cancer cells.<sup>[22–25]</sup> The antitumoral activity of the monocyclic sesquiterpene dienone zerumbone has been related to its ability to selectively inhibit cancer cell viability/proliferation, and to induce apoptosis, mitochondrial depolarization, accumulation of cytosolic lipid droplets, and changes in lipid profile and cell membrane organization/protein

dynamics.<sup>[22,39]</sup> The polymethoxylated flavones eupatilin<sup>[23,40]</sup> and artemetin<sup>[24,41]</sup> target cancer cells inducing cytotoxicity, cell cycle arrest, apoptosis, mitochondrial dysfunction, and lipid profile modulation. Recent research showed that C- and O-prenylation significantly increased the cytotoxic effect, the capacity to affect lipid profile, and the bioavailability of artemetin in cancer HeLa cells.<sup>[25]</sup> Zerumbone and eupatilin induced a marked decrease of 18:1 n-9 and the accumulation of 18:0, compatible with a potential drug-induced inhibition of the enzyme SCD.<sup>[22,23]</sup> The reduction of palmitic acid induced by both compounds was compatible with a potential abrogation of lipid synthesis.<sup>[22,23]</sup> Similarly, the incubation of cancer HeLa cells with artemetin induced a dose-response decrease in the cell level of 18:1 n-9, 16:1 n-7, and 16:0,<sup>[24]</sup> while the cell treatment with its prenylated derivatives induced a marked reduction of 18:1 n-9 and 16:1 n-7 levels together with an increase in the level of 16:0, 18:0, and several PUFA.<sup>[25]</sup> The main FA ratios were calculated in HeLa control cells and cells treated with the antitumoral compounds zerumbone, eupatilin, artemetin, its derivatives 8-prenyl artemetin, and 5-O-prenyl artemetin obtained from different experimental sets.<sup>[22–25]</sup> PCA, a chemometric technique amply used for pharmaceutical applications,<sup>[42]</sup> separately performed on FA and FA ratio data showed similar clustering of HeLa cell samples concerning the type and dose of treatment, validating their potential as alternative biomarkers for comparing the effect on FA metabolism of different treatments in the same cancer cell line. Moreover, the differences between treatments and for each treatment between the different tested doses, were quantitatively evaluated by the calculation of the graphical distances in the PCA plots. We previously used this quantitative method for the comparative evaluation of the composition of vegetable essential and fixed oils obtained by supercritical extraction and conventional techniques.<sup>[26]</sup> The multivariate analysis of cell FA ratios and calculated distances led practically to the same results as the analysis of the full FA data set PCA, validating the potential role of FA ratios as cell metabolic parameters for comparative evaluation of different nutritional and pharmacological treatments.

## 5. Conclusion

We explored in the cell culture system, through a biochemical and chemometric approach, the use of the cell FA ratio profile as a data set alternative to the cell FA profile. Our results qualified the pool of FA ratios, calculated between the most abundant cellular FA, as useful parameters for cell characterization, discrimination between normal and cancer cells, and the quantitative comparison of different drug treatments in the same cell line. Altogether, these findings demonstrate that the FA ratio profile is a cell-specific fingerprint, characterized by reproducibility across intra-laboratory conditions. The definition of the FA ratio profile for a specific cell line cultured in standardized growth conditions could facilitate the comparison of cell data sets across different laboratories in nutritional, metabolic, and pharmacological studies.

## Supporting Information

Supporting Information is available from the Wiley Online Library or from the author.

## Conflict of Interest

The authors declare no conflict of interest.

## Author Contributions

Conceptualization, methodology, validation, formal analysis, investigation, resources, data curation, visualization, supervision, writing—original draft, supervision, writing—review & editing: A.R. Methodology, investigation, resources, writing—review & editing: M.N. Methodology, investigation, resources, writing—review & editing: F.P. Methodology, validation, formal analysis, data curation, visualization, writing—review & editing: C.P.

## Data Availability Statement

The data supporting this study's findings are available from the corresponding author upon reasonable request.

## Keywords

anticancer drugs, cells, fatty acid ratios, lipid profile modulation, principal component analysis

Received: July 13, 2022  
Revised: December 19, 2022  
Published online:

- [1] C. R. Santos, A. Schulze, *FEBS J.* **2012**, *279*, 2610.
- [2] Z. Wu, G. I. Bagarolo, S. Thoröe-Boveleth, J. Jankowski, *Adv. Drug Delivery Rev.* **2020**, *159*, 294.
- [3] N. Koundouros, G. Pouligiannis, *Br. J. Cancer* **2020**, *122*, 4.
- [4] C. Ferreri, A. Masi, A. Sansone, G. Giacometti, A. V. Larocca, G. Menounou, R. Scanferlato, S. Tortorella, D. Rota, M. Conti, S. Deplano, M. Louka, A. R. Maranini, A. Salati, V. Sunda, C. Chatgililoglu, *Diagnostics* **2016**, *7*, 1.
- [5] M. Ibarguren, D. J. López, P. V. Escribá, *Biochim. Biophys. Acta, Biomembr.* **2014**, *1838*, 1518.
- [6] Y. K. Denisenko, O. Y. Kytikova, T. P. Novgorodtseva, M. V. Antonyuk, T. A. Gvozdenko, T. A. Kantur, *J. Obes.* **2020**, 5762395.
- [7] S. R. Nagarajan, L. M. Butler, A. J. Hoy, *Cancer Metab.* **2021**, *9*, 2.
- [8] Q. Liu, Q. Luo, A. Halim, G. Song, *Cancer Lett.* **2017**, *401*, 39.
- [9] X. Luo, C. Cheng, Z. Tan, N. Li, M. Tang, L. Yang, Y. Cao, *Mol. Cancer* **2017**, *16*, 76.
- [10] A. Mika, K. Duzowska, L. P. Halinski, A. Pakiet, A. Czumaj, O. Ros-tkowska, M. Dobrzycka, J. Kobiela, T. Sledzinski, *Front. Oncol.* **2021**, *11*, 689701.
- [11] A. Bitencourt, V. Sevilimedu, E. A. Morris, K. Pinker, S. B. Thakur, *Diagnostics* **2021**, *11*, 564.
- [12] Z. Tracz-Gaszewska, P. Dobrzym, *Cancers* **2019**, *11*, 948.
- [13] V. Fritz, Z. Benfodda, C. Henriquet, S. Hure, J. P. Cristol, F. Michel, M. A. Carbonneau, F. Casas, L. Fajas, *Oncogene* **2013**, *32*, 5101.
- [14] L. M. Butler, Y. Perone, J. Dehairs, L. E. Lupien, V. de Laet, A. Talebi, M. Loda, W. B. Kinlaw, J. V. Swinnen, *Adv. Drug Delivery Rev.* **2020**, *159*, 245.
- [15] D. Lv, Z. Hu, L. Lu, H. Lu, X. Xu, *Oncol. Lett.* **2017**, *14*, 6999.
- [16] A. Verma, M. Verma, A. Singh, in *Animal Biotechnology*, 2nd ed. (Eds: A. S. Verma, A. Singh), Elsevier, Amsterdam, the Netherlands **2020**, p. 269.
- [17] H. Barosova, K. Meldrum, B. B. Karakocak, S. Balog, S. H. Doak, A. Petri-Fink, M. J. D. Clift, B. Rothen-Rutishauser, *Toxicol. In Vitro* **2021**, *75*, 105178.

- [18] M. Baker, *Nature* **2016**, 537, 433.
- [19] M. Graeve, M. J. Greenacre, *Limnol. Oceanogr.: Methods* **2020**, 18, 196.
- [20] A. M. Rizzo, G. Montorfano, M. Negrone, L. Adorni, P. Berselli, P. Corsetto, K. Wahle, B. Berra, *Lipids Health Dis.* **2010**, 9, 7.
- [21] X. Meng, N. H. Riordan, H. D. Riordan, N. Mikirova, J. Jackson, M. J. González, J. R. Miranda-Massari, E. Mora, W. T. Castillo, *P. R. Health Sci. J.* **2004**, 23, 103.
- [22] A. Rosa, D. Caprioglio, R. Isola, M. Nieddu, G. Appendino, A. M. Falchi, *Food Funct.* **2019**, 10, 1629.
- [23] A. Rosa, R. Isola, F. Pollastro, P. Caria, G. Appendino, M. Nieddu, *Food Funct.* **2020**, 11, 5179.
- [24] A. Rosa, R. Isola, F. Pollastro, M. Nieddu, *Fitoterapia* **2022**, 156, 105102.
- [25] S. Salamone, M. Nieddu, A. Khalili, A. Sansaro, E. Bombardelli, A. Rosa, F. Pollastro, *Chem. Phys. Lipids* **2021**, 240, 105137.
- [26] A. Piras, S. P. C. Piras, A. Rosa, *J. Food Sci. Technol.* **2021**, 56, 4496.
- [27] F. F. Eiriksson, M. K. Nøhr, M. Costa, S. K. Bödvarsdóttir, H. M. Ögmundsdóttir, M. Thorsteinsdóttir, *PLoS One* **2020**, 15, e0231289.
- [28] R. Bro, A. K. Smilde, *Anal. Methods* **2014**, 6, 2812.
- [29] A. Rosa, A. Piras, M. Nieddu, D. Putzu, F. Cesare Marincola, A. M. Falchi, *Food Funct.* **2016**, 7, 4092.
- [30] G. Maulucci, O. Cohen, B. Daniel, A. Sansone, P. I. Petropoulou, S. Filou, A. Spyridonidis, G. Pani, M. De Spirito, C. Chatgialoglu, C. Ferreri, K. E. Kyreos, S. Sasson, *Free Radic. Res.* **2016**, 50, S40.
- [31] H. Sunshine, M. L. Iruela-Arispe, *Curr. Opin. Lipidol.* **2017**, 28, 408.
- [32] F. Rey, M. Greenacre, G. M. Silva Neto, J. Bueno-Pardo, M. R. Domingues, R. Calado, *Mar. Environ. Res.* **2022**, 173, 105517.
- [33] P. L. Else, *Prog. Lipid Res.* **2020**, 77, 101017.
- [34] H. Tallima, R. El Ridi, *J. Adv. Res.* **2018**, 11, 33.
- [35] P. C. Calder, *Ann. Nutr. Metab.* **2016**, 69, 7.
- [36] Y. Fu, T. Zou, X. Shen, P. J. Nelson, J. Li, C. Wu, J. Yang, Y. Zheng, C. Bruns, Y. Zhao, L. Qin, Q. Dong, *MedComm* **2021**, 2, 27.
- [37] P. C. Theodoropoulos, S. S. Gonzales, S. E. Winterton, C. Rodriguez-Navas, J. S. McKnight, L. K. Morlock, J. M. Hanson, B. Cross, A. E. Owen, Y. Duan, J. R. Moreno, A. Lemoff, H. Mirzaei, B. A. Posner, N. S. Williams, J. M. Ready, D. Nijhawan, *Nat. Chem. Biol.* **2016**, 12, 218.
- [38] A. Pakiet, J. Kobiela, P. Stepnowski, T. Sledzinski, A. Mika, *Lipids Health Dis.* **2019**, 18, 29.
- [39] K. Kalantari, M. Moniri, A. Boroumand Moghaddam, R. Abdul Rahim, A. Bin Ariff, Z. Izadiyan, R. Mohamad, *Molecules* **2017**, 22, 1645.
- [40] B. Nageen, I. Sarfraz, A. Rasul, G. Hussain, F. Rukhsar, S. Irshad, A. Riaz, Z. Selamoglu, M. Ali, *J. Asian Nat. Prod. Res.* **2020**, 22, 1.
- [41] J. F. Ferreira, D. L. Luthria, T. Sasaki, A. Heyerick, *Molecules* **2010**, 15, 3135.
- [42] I. Singh, P. Juneja, B. Kaur, P. Kumar, *ISRN Anal. Chem.* **2013**, 2013, 795178.